Acta Materialia 142 (2018) 58–70

Contents lists available at ScienceDirect

Acta Materialia

journal homepage: www.elsevier.com/locate/actamat

Full length article

Effect of plastic anisotropy on the deformation behavior of bicrystalline aluminum films – Experiments and modeling

Ehsan Izadi, Saul Opie, Harn Lim, Pedro Peralta, Jagannathan Rajagopalan*

Mechanical and Aerospace Engineering, School for Engineering of Matter, Transport and Energy, Arizona State University, Tempe, AZ 85287, USA

ARTICLE INFO

Article history:
Received 1 June 2017
Received in revised form
12 September 2017
Accepted 17 September 2017
Available online 20 September 2017

Keywords:
Strain rate sensitivity
Plastic anisotropy
Bauschinger effect
Thin films
Strain hardening

ABSTRACT

We investigated the effect of texture-induced plastic anisotropy on the deformation behavior of ultrafine-grained aluminum films with a bicrystalline texture (two grain variants). The films were uniaxially loaded along two different directions such that the heterogeneity in the plastic behavior of the two grain variants due to plastic anisotropy was minimized along one direction and maximized along the other. The bicrystalline films show smaller strain rate sensitivity and hysteresis of stress-strain response when they are deformed along the direction that minimizes plastic heterogeneity compared to the direction that maximizes it. Notable differences in flow stress and residual hardening were also found for the two loading directions. To quantitatively understand the effect of plastic anisotropy, we simulated the response of the films using three-dimensional finite elements with a microstructurally explicit model built from TEM automated crystal orientation mapping of the samples that includes a grain boundary region, along with crystal plasticity and anisotropic elasticity. The simulations reveal markedly different distribution of stresses and strains in the two grain variants when loading is performed along the two directions, which can be directly related to the ratio of Schmid factors of their most active slip systems.

1. Introduction

The processing and characterization of ultrafine-grained (UFG) and nanocrystalline (NC) metals and alloys have attracted significant attention in recent years [1,2], because of their superior mechanical properties such as high strength, enhanced corrosion resistance and improved fatigue strength compared to coarse-grained (CG) materials [1,3–6]. In addition, UFG/NC metals exhibit certain unusual characteristics as compared to their CG counterparts, like high strain rate sensitivity, plastic strain recovery and early Bauschinger effect (BE), which have been attributed to changes in the underlying deformation mechanisms [7–13]. Initial research on the deformation behavior of UFG/NC metals focused mainly on the effect of mean grain size on strength and ductility, and the validity of the Hall–Petch relation [14,15], in the UFG/NC regime. Later studies have explored in detail the effect of sample dimensions as well as other microstructural parameters on the flow stress, strain hardening behavior and strain rate sensitivity [16–21]. There has also been a substantial effort to characterize and improve the mechanical and thermal stability of UFG/NC microstructures [22–24].

More recently, texture has been shown to significantly influence the mechanical response of thin UFG/NC metal films [25]. Torre et al. have reported that NC Ni foils with different textures show a variation in the yield stress and ultimate strength [26]. UFG Al films with different textures but similar thickness and mean grain size show substantial changes in BE, and strain rate sensitivity of flow stress [7,27,28]. However, the effect of plastic anisotropy on the deformation behavior of UFG/NC metal films has received relatively little attention. Plastic anisotropy, which can be induced in UFG/NC films as a result of crystallographic texture, can affect the hardening behavior and stress distribution in the grains and influence the extent of inelastic strain recovery. While some studies have considered the effect of Schmid factor variation [25,29–32] on the stress-strain response of both CG and UFG/NC materials, a systematic study of these effects on UFG metal films has been lacking.

To address this issue, we performed monotonic deformation experiments at different strain rates and quasi-static cyclic loading experiments on two sets of UFG aluminum films with identical bicrystalline texture (two grain variants). The films were uniaxially loaded in two different directions with respect to the main crystallographic axes of the bicrystalline texture, such that the

* Corresponding author.
E-mail address: jrajago1@asu.edu (J. Rajagopalan).

https://doi.org/10.1016/j.actamat.2017.09.038
1359-6454/

heterogeneity in the plastic behavior of the two grain variants due to plastic anisotropy was minimized along one direction and maximized along the other direction. The bicrystalline films showed ~20% lower strain rate sensitivity (SRS) when loaded along the direction that minimizes heterogeneity due to plastic anisotropy compared to loading along the direction that maximizes the effect. Cyclic loading-unloading experiments also show significantly less hysteresis in the stress-strain response when the loading is performed along the direction that minimizes heterogeneity due to plastic anisotropy.

To quantitatively understand the effect of plastic anisotropy, we simulated the response of the films using three-dimensional finite elements with a microstructurally explicit model built from automated crystal orientation mapping of the samples along with crystal plasticity and anisotropic elasticity. The simulations quantitatively predict the macroscopic response of the bicrystalline films and provide insights into the evolution of plastic anisotropy-induced stress heterogeneities within the two grain variants, as well as the potential role of the compliance at the grain boundaries.

2. Experimental details

2.1. Thin film synthesis

Two bicrystalline aluminum films (240 nm and 180 nm thick) were deposited on Si (100) wafers using DC magnetron sputtering. The native silicon dioxide layer on the Si wafers was removed through hydrofluoric acid etching and the wafers were immediately transferred to the sputtering chamber (AJA International) to avoid regrowth of the oxide layer. The sputtering chamber was evacuated to a base pressure of $\sim 10^{-7}$ Torr prior to deposition and both films were deposited at a rate of 5.5 nm/min. The Al films grew in a heteroepitaxial manner with the following orientation relationship: Al(110)//Si(001), Al[001]//Si[$1\bar{1}0$] and Al(110)//Si(001), Al [001]//Si[110] [33], leading to two grain families with (110) out-of-plane texture that are rotated 90° in-plane with respect to each other.

2.2. Microstructural characterization and sample fabrication

The microstructures of the films were examined through bright-field transmission electron microscopy (TEM) and automated crystal orientation mapping (ACOM) in the TEM (ACOM-TEM). For the ACOM-TEM measurements, an electron probe with ~1 nm diameter was generated using spot size 4 and 10 μm C2 aperture in a JEOL 200 F ARM TEM. Spot diffraction patterns were obtained from the samples with a 10 nm step size using an electron beam precession angle of 0.4° and a camera length of 120 mm. The acquired ACOM-TEM data was indexed by matching the spot diffraction patterns with a bank of templates for aluminum using the Nanomegas ASTAR™ software package to generate the grain orientation maps. Fig. 1 shows bright-field TEM images of the two Al films, indicating a columnar grain structure. The 180 nm thick film had a mean grain size of 228 nm, whereas the 240 nm thick film had a mean grain size of 275 nm. Selected area diffraction (SAD) patterns taken along the [110]-zone axis (Fig. 2a) showed that only two grain variants, which can be obtained by a 90° rotation with respect to each other in-plane, were present in the films. A schematic representation of these variants is shown in Fig. 2b. The (110) out-of-plane texture and the bicrystalline microstructure of the films were also confirmed by ACOM-TEM measurements (Fig. 2c and d).

After the films were deposited, dog-bone shaped freestanding samples were co-fabricated with a micro-electro-mechanical-system (MEMS) based tensile testing device (Fig. 3a) using microfabrication techniques outlined in Ref. [34]. A piezoelectric actuator (Physik Instrumente) was used to load the MEMS device and a CMOS camera (Thor Labs) was used to acquire optical images of the gauges, G1, G2 and G3, in the device. The force and deformation on the sample during the cyclic loading experiments were obtained by measuring the displacement of the gauges using a custom MATLAB™ program, which tracks prescribed features across a series of images using cross-correlation techniques. The displacement of G1 with respect to G2 ($\Delta X_{12} = X_{G1} - X_{G2}$) represents the deformation of the sample, from which the sample strain is obtained. The deflection of the force-sensing beams is given by the displacement of G2 with respect to G3 ($\Delta X_{23} = X_{G2} - X_{G3}$). As evident from the equivalent mechanical model of the device, the sample is arranged in series with the force-sensing beams (Fig. 3b) and, hence the force on sample and the force-sensing beams is the same. The stiffness of the force-sensing beams (K) was measured in a separate experiment after the sample had fractured. K multiplied by ΔX_{23} gives the force and, thus, the stress on the sample. For measuring the stress-strain response during monotonic loading experiments at different strain rates, a slightly modified MEMS device along with an external micro load cell was used, as described in Ref. [27].

To determine the error in strain measurement, we displaced the gauges by a prescribed amount and recorded images before and

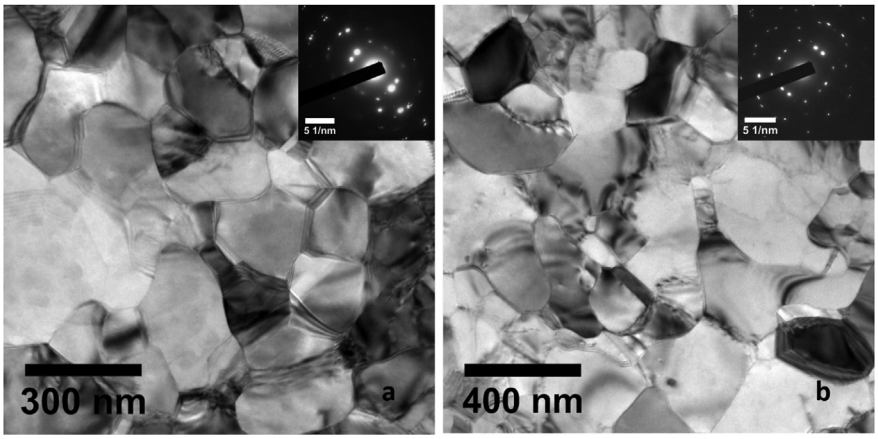

Fig. 1. (a) Bright-field TEM image of a 180 nm thick, bicrystalline aluminum film with a mean grain size of 228 nm. (b) Bright-field TEM image of a 240 nm thick, bicrystalline aluminum film with a mean grain size of 275 nm. The selected area diffraction (SAD) patterns for both films (insets in (a) and (b)) show the (110) out of plane texture. The two in-plane variants that can be obtained by a 90° rotation with respect to each other about the out-of-plane direction.